

## **Acoustic emission characterization of intralaminar damage in composite laminates**

**A.M. Abad Blazquez, M.Herraiez Matesanz, C. Navarro Ugena**

Departamento de Mecánica de Medios Continuos y Teoría de Estructuras, Universidad  
Carlos III de Madrid, España

**Ever J. Barbero,**

Department of Mechanical and Aerospace Engineering, West Virginia University, USA  
Departamento de Mecánica de Medios Continuos y Teoría de Estructuras, Universidad  
Carlos III de Madrid, España

### **ABSTRACT**

A novel application of the acoustic emission technique is developed in this manuscript in order to identify intralaminar matrix cracks continuously during uniaxial extension of laminated composites. The position of the cracks along the specimen length is found and correlated with X-ray radiography.

**KEYWORDS:** Acoustic emissions, damage.

### **1. INTRODUCTION**

Intralaminar damage in laminated composites is the first mode of damage encountered in most applications of laminated composites. Furthermore, it precipitates other catastrophic modes of failure, such as delaminations and fiber fracture. Also, intralaminar cracks are responsible for drastic increases of permeability of the laminate that compromises the imperviousness of the shell. Moreover, matrix cracks expose the fibers and the interlaminar interfaces to environmental attack, such as moisture, and thermomechanical loading by cryofluids. Therefore, accurate prediction of initiation and evolution of intralaminar matrix cracks is fundamental for the prediction of ultimate material and structural strength, fatigue life, and so on.

All predictive models available rely on material properties such as the intralaminar fracture toughness in opening and shear modes to predict the initiation and evolution of intralaminar crack density [1,2]. Such material properties are difficult to measure.

Therefore, the objective of this work is to develop an acoustic emissions methodology to measure the crack density as a function of applied strain. AE events are discriminated from noise, and/or other type of events, by using two metrics developed in this work, in such a way that events correspond fairly closely to events discerned by direct observation using X-ray radiography.

## 2. MATERIALS AND METHODS

During sample processing and fabrication, our aim was to eliminate variability as much as possible [3,4]. Flat laminates were produced by hand layup, vacuum bagging, and oven cure and post-cure using prepreg MTM45-1/IM7-GP-145-32%RW carbon/epoxy. The fiber is IM7 with fiber area weight FAW=145 g/m<sup>2</sup>, fiber volume fraction  $V_f=58.72\%$ , and nominal cured ply thickness CPT=0.140 mm. Four laminates were produced as shown in Table 1.

Table 1. Laminates.

Label	LSS
A	[0/90 <sub>4</sub> ] <sub>s</sub>
B	[±25/90 <sub>5</sub> ] <sub>s</sub>
C	[0/±55/0 <sub>1/2</sub> ] <sub>s</sub>
D	[0/±70/0 <sub>1/2</sub> ] <sub>s</sub>

The laminates were vacuum bagged to 28 mm Hg (minimum), maintaining the vacuum during the entire curing and post-curing process. Compliance regarding curing time, vacuum, and temperature were assured by continuous data logging during the entire process. Curing was done for 4 h at 120 °C followed by post-curing at 180 °C for 2 h. Temperature was ramped at 3 °C/min from room temperature ambient (RTA) to 120 °C and then at 0.3 °C/min from 120 °C to 180 °C. Cooling was done at -2 °C/min. Surface texture was achieved on both sides of the plates by using a peel ply. During layup, debulking was performed every 4 or 5 plies.

The first specimen of each laminate was tested in three or four successive phases: phase 'a' followed by phase 'b', followed by phase 'c', and in some cases followed by phase 'd'. The remaining specimens were tested without interruption. Samples, specimens, and test phases are identified by a 3-letter code. The first letter indicates the sample, which is the laminate type (A, B, C, D). The second identifies the number of specimen from a given sample. The third identifies the phase of the test (a, b, c, d).

The specimens were prepared following ASTM D3039. They were cut from the plates using a Norton diamond wheel SD100-R100B99-1/4, and the cut edges were sanded with 80 grit followed by 220 grit sandpaper. Fiberglass tabs, 51 mm long, were bonded using general purpose Epoxy adhesive, to the ends of the specimens to protect the specimen from the grips of the Universal Testing System.

Two microphones were attached using RTV sealant Permatex 81160(26B), at a distance centre to centre of 146 mm. The gage section of 102 mm was marked with a short length copper wire held with adhesive tape, so that they are visible in the X-ray pictures.

All specimens were instrumented with MM C2A-06-250LW-350 strain gages on one side only to measure the axial strain along the specimen's length.

Displacement controlled loading, 0.127 mm/min was provided using a MTS 810 universal testing system (UTS) with Model 647 wedge grips, FlexTest SE controller,

and TestWare software. The controller was custom interfaced with a Vishay MM 2100 system to condition the strain gage signal and with the AE system. All the signals, load, stroke, and strain were fed into the AE system for simultaneous data logging.

### 2.1. Acoustic Emissions

The acoustic emissions system (AE) has the following components:

- Data acquisition and processing card Mistras PCI-2 (18 bit AE), with 1kHz-3MHz bandwidth.
- Two microphones WD S/N FR 05 & 06 and two voltage preamplifiers 2/4/6.
- Software AEwin PCI-2.

Using two microphones, the observation region is confined inside the specimens, not including the ends of the specimens and the grips. The advantages of this configuration are:

- External events are discarded, so there is no need to filter them.
- Inaccuracies associated with the proximity of the acoustic receivers are minimized.
- In any case, the maximum observation length on the X-rays is 10.2 cm, so observing a longer region by AE has no benefit.
- Reducing the observation region to 102 mm poses no significant inaccuracy in the results because the parameter being measured is the crack density (number of cracks / mm), for which an observation length of 102 mm contains many cracks.

In order to localize the cracks, i.e., to find the position of events between the two microphones, the following assumptions are accepted:

- Uniaxial propagation is justified by the slenderness of the specimens ( $L=267$  mm,  $W=19$  mm,  $t<2.8$  mm) with  $L/W>10$  and  $L>>t$ .
- Matrix cracks propagate suddenly over the entire width of the specimen, as supported by theoretical arguments [5, Sect. 7.2.1], and experimental evidence in this work and elsewhere.
- The wave speed is uniform along the length of the specimen and throughout testing because wave speed is dominated by the laminas that do not experience damage during testing, notably 0-deg laminas. Such wave speed was determined experimentally for each specimen before testing and corroborated as per ASTM E976.

Finally, the AE system was set up to receive and record the load signal from the UTS (2000 LbF/V) and the strain conditioning unit (2000 microstrain/V, both through differential +/-10 V signals. The preamplification was fixed at 40 db.

### 2.2. X-ray radiography

X-ray radiographs were taken off line, at discrete load intervals, using a HP Faxitron 43855A. To contrast the cracks, a penetrating solution was applied prior to each X-ray exposure. The solution was prepared according to the following recipe: 60 g of pulverized  $ZnI_2$ , 8 ml distilled water, 10 ml isopropyl alcohol, and 3 ml of Kodak Photo-Flo 200. Before X-ray exposure, penetrating solution was applied to the edges of the specimens using a craft paintbrush.

Exposure and development time must be determined by trial and error for each type of film and X-ray machine. We used Polaroid/Fujifilm FP-100C45 (102 x 127 mm)

professional instant colour film. We obtained good results with 90 sec development time at 22 °C. The exposure time is a function of the thickness of the specimens. For samples A and B, containing 10 and 14 plies, respectively, we used 2 min exposure. For samples C and D, both containing 19 plies, we used 2:20 min exposure, in all cases at 30kVp power setting. A film holder was used to keep the film flat. Most film holders have a metallic backing, which must be removed. Then, the specimen is placed on top of the holder, between the film and the X-ray source.

### 3. CALIBRATION

AE captures many events, but not all events correspond to matrix cracks. For each event, AE provides a number of characteristics, including: Energy, Amplitude, Ramp time, Duration, Counter, Frequency centroid, Peak frequency, Mean frequency, AE threshold (45 dB).

The objective of the work described in this section is to develop a metric that allows to differentiate the events that corresponds to cracks from those that do not. This is done by matching those AE events that correspond to cracks observed on radiography (Fig. 1) and then looking at the characteristics of those events. The matching is provided by the location, which can be obtained from both the AE data and the X-ray.

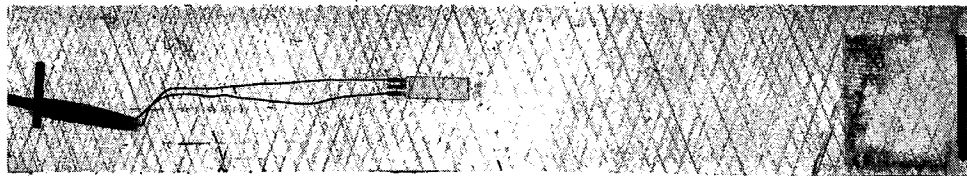


Figure 1. X-ray of specimen  $[0/\pm 70/0_{1/2}]_s$ , load stage c.

Once the cracks can be counted from the AE event log, the crack density is computed as number of cracks detected divided by the observation gage (102 mm).

#### 3.1. Predominant mode I fracture

Only fracture mode I (opening) is active in laminates A and B, where only the transverse center lamina sustains matrix cracking. To investigate the characteristics of matrix cracks, specimen A-1 was loaded in three phases: a, b, and c. At the end of each phase, the specimen was removed from the UTS and X-rayed. From the radiography, the cracks are clearly identifiable.

The position of all cracks seen on the X-ray were found in the AE event log by matching their position along the length of the specimen. Next, all the characteristics of the AE events were studied, observing that the event energy provided the most discriminating quality between events that correspond to cracks and those that do not.

Events outside the range do not correspond to matrix cracks. Therefore, for this LSS, any event within that energy range is considered to be a crack. This allows us to perform additional tests where crack density is measured continuously during loading, without stopping at discrete intervals of load to X-ray the specimen. The main advantage is that a test can be completed in a few minutes instead of several hours.

A few cracks were missed by the AE identification procedure so far described. The effectiveness of this methodology is quantified by the correspondence coefficient, defined as follows:

$$c = \frac{|Xray\ cracks - AE\ cracks|}{Xray\ cracks}$$

which for sample A-1 is  $c=95.18\%$ . That means that 95% of the cracks seen on the X-ray pictures are identified by the AE procedure described so far. There are many events under the lower energy threshold (3 mJ), which are thought to be noise. Also, there are a few above the upper limit (45 mJ), which may be fiber breaks.

For specimen B-1, an energy range (3—37 mJ) was satisfactory but using the range of specimen A-1 (3—45 mJ) did not introduce any error, so the later was used. Again, only a few non-crack events corresponded to energies higher than the upper limit (45 mJ) and the majority of the non-crack events had energies below the lower threshold (3 mJ).

An alternative criterion is proposed, called P-criterion, which also provides very good discrimination of events. It is defined as the product of the amplitude times the energy of the event, as

$$P_i = A_i \int_{t_0}^{t_f} I_i(t) dt$$

where  $A_i$  is the maximum amplitude and  $I_i(t)$  is the intensity of the event. The P-criterion provides more contrast than the energy criterion according to the brittleness of the tested material. With it, events with very low intensity and long duration, that might have significant energy, can be discarded. Also, events with low duration but very high amplitude, that might have low energy, become discernible and they can be kept. Overall the P-criterion did a better job than the energy criterion at identifying cracks that were also observed in the X-ray photographs.

Using the same data discussed so far, the range that captures all the cracks is (270—4400 mJ dB). The correspondence coefficient for specimens A-1 and B-1, using E-criterion (energy) are  $c=95.18\%$  and  $c=97.44\%$ , while using P-criterion are  $c=96.38\%$  and  $c=97.44\%$ , respectively. Therefore, either criterion can be applied for transverse matrix cracks, but we shall see that the P-criterion is more effective when the cracks develop at an angle, in laminates C and D.

Laminated A-2, A-3, B-2, B-3, were tested without stops, and with X-rays taken only at the end of the tests. The AE event log was filtered using the P-criterion. The X-ray count at the end of each test is very close to the AE count, although it is quite difficult to count cracks on the X-ray photograph taken at the end of the test because of the large number of very closely spaced cracks that has to be counted.

### 3.2. Predominant mixed mode fracture

Laminates C and D have two symmetric sets of angle plies. Under uniaxial extension, cracks develop in a mixed-mode condition involving mode I (crack opening) and mode

II (crack shear). Mode III (crack tearing) does not participate because tearing is restrained by the adjacent laminas, i.e., there cannot be out-of-plane displacements of the faces of the crack. Further, since there are four cracking laminas, the crack density is calculated as  $n/4L$ , where  $n$  is the number of cracks discerned by the AE system, and  $L=102$  mm is the observation length.

As in previous section, one specimen of each laminate was used to find the range of P-criterion that encompasses those events corresponding to cracks observed in X-ray photographs.

For laminate C, the thresholds for which 99% of cracks were identified by AE system were 18 – 78 mJ dB. In case of laminate D, these thresholds were found to be at 75 – 280 mJ dB reaching a correspondence coefficient of 98% against X-ray pictures.

Laminates C-2, C-3, D-2, D-3, were tested without stops. X-rays were taken only at the end of the test. The X-ray count at the end of each test is very close to the AE count, although it is quite difficult to count cracks on the X-ray photograph taken at the end of the test because of the large number of very closely spaced cracks that has to be counted. The AE event log was filtered using the P-criterion.

According to the threshold values for every LSS, the amount of energy released when matrix cracks appear depends on the number of cracking laminae and the orientation.

#### 4. CONCLUSIONS

The acoustic emissions technique can be used effectively to record crack density vs. strain without having to stop to count cracks at discrete intervals using techniques such as X-ray or microscopy. Further, the proposed methodology can identify cracks in angle-ply laminas, which are very difficult if not impossible to see with microscopy. It was observed that the strain rate has an effect on crack density rate, and thus it is suggested as a topic for further study. A drawback of the proposed method is that the AE threshold parameters need to be identified for each LSS by initial comparison with X-ray.

#### BIBLIOGRAPHY

1. BARBERO E.J., F. A. COSSO, R. ROMAN, T. L. WEADON, Determination of Material Parameters for Abaqus Progressive Damage Analysis of E-Glass Epoxy Laminates, *Composites Part B*, 46(March 2013), 211–220.
2. BARBERO E.J., CORTES D.H. (2010). A mechanistic model for transverse damage initiation, evolution, and stiffness reduction in laminated composites, *Composites Part B*, 41, pp. 124-132.
3. ABAD BLÁZQUEZ, A.M., Experimental Determination of Transversal Matrix Damage Using Acoustic Emission, PFC Ingeniería Industrial, UC3M, Spain (2012).
4. HERRÁEZ MATESANZ, M., Determinación Experimental de la Tenacidad de Fractura Intralaminar en Materiales Compuestos Laminados, PFC Ingeniería Industrial, UC3M, Spain (2012).
5. BARBERO E.J., Introduction to composite Materials Design—Second Edition, CRC(2010).